This article has been accepted for publication in a future issue of this journal, but has not been fully edited. Content may change prior to final publication. Citation information: DOI 10.1109/TAP.2017.2715366, IEEE Transactions on Antennas and Propagation

Stochastic Solutions to Rough Surface Scattering using the Finite Element Method

Uday K Khankhoje* *Senior Member, IEEE,* and Shreyas Padhy†

***Abstract*—We propose stochastic solutions to the scattering of electromagnetic waves from penetrable randomly rough surfaces using the vector based finite element method (FEM). The random nature of the surface requires the computation to be performed on multiple surface instances. We propose a mesh deformation scheme which allows the use of a single FEM mesh for computing ensemble averaged quantities. This scheme is used to perform Monte Carlo (MC) iterations, which is much faster than conventional techniques where a different mesh is utilized for each surface instance. This scheme also allows for MC-free formulations of the problem; in the first kind, we expand the solution in a stochastic basis using the concept of generalized Polynomial chaos obtain ensemble averaged quantities. This results in a larger set of equations that need to be solved just once. In the second kind —the stochastic collocation method— we run the deterministic solver at certain specified points in the random domain corresponding to the rough surface description. We compare these results with those obtained by MC iterations, outline the computational costs and convergence behavior. We find that stochastic methods are ideal for surfaces with large correlation lengths. For other parameters, the Monte Carlo approach is preferable.**

Keywords: Electromagnetic scattering by rough surfaces; finite element methods; monte carlo methods; uncertainty

I. Introduction

Motivation: The problem of computing the scattering of electromagnetic waves from randomly rough surfaces is of paramount interest in microwave remote sensing of natural surfaces such as land and ocean. Remote sensing missions such as the Soil Moisture Active Passive (SMAP) mission [1] (and many others) attempt to recover quantities of interest (QoI) such as soil moisture, ocean salinity, freeze/thaw soil states, etc. through the measurement of scattered radar waves. However, it is very difficult to separate the impact on the radar cross-section (RCS) of these QoI, from the impact due to surface roughness.

In the study of rough surface scattering (see [2] for a review) it is the case that the surface is modelled as a stochastic process, and many degrees of freedom are required to characterize it. As a result, any QoI such as those indicated above, end up living inside a high dimensional parameter space. Thus, the inverse problem – that of computing the QoI directly from remotely sensed data – becomes extremely challenging. As an alternative, the forward problem – finding the scattered field for a given geometry – is pre-computed for various plausible geometries and the results subsequently compared with measured data [3] to infer the QoI. Apart from the motivation from remote sensing, the problem of electromagnetic rough surface scattering (and the closely related acoustic version) in a computationally efficient manner is a challenging and interesting research problem in its own right. In this paper, we report recent advances in addressing this challenge via the finite element method (FEM) in a two-dimensional setting.

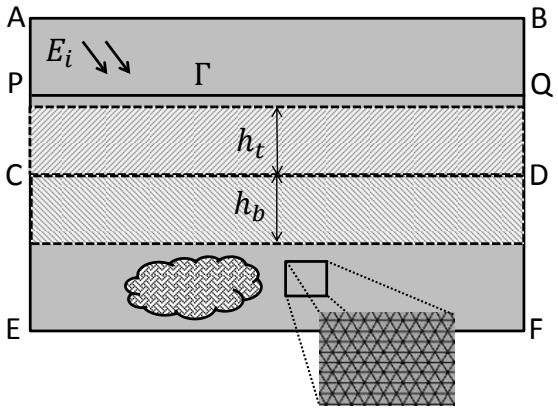

Fig. 1: Schematic of computational domain for the FEM. CD is the (flat) interface between two half-spaces; vacuum above and a heterogeneous substrate below. An incident field E_i falls on this interface; the contour Γ is used for evaluating the radar cross-section; the shaded regions (of height h_t, h_b) represent the regions within which the mesh is deformed in response to a rough surface; a possible heterogeneity in the substrate is indicated in the lower half of the substrate, and the inset (bottom right) shows a typical tessellation of the domain into finite elements. In this paper, $AP = PC = CE/2 = 0.5\lambda$, $h_t = 0.4\lambda$, and $h_b = 0.5\lambda$.

Problem description: In particular, we detail a stochastic solution approach that is free from Monte Carlo iterations. This is accomplished by expanding the rough surface in a stochastic basis, and then embedding this expansion into the FEM itself. This is made possible by means of a smooth mesh deformation scheme, where a subset of the nodes of a finite element tessellation are moved in response to the coordinates describing a rough surface. We use the FEM primarily because of the versatility of this tool, since heterogeneity in the substrate is easily modelled with the FEM. This heterogeneity could arise, for instance, due to a buried object, depth-dependent soil moisture, etc. (see the schematic in Fig. 1 for an illustration of a typical scattering geometry). Over the last couple of decades, integral equation based methods

Electrical Engineering*, Indian Institute of Technology Madras, Chennai, India 600036; Physics†, Indian Institute of Technology Delhi, New Delhi, India 110016. *Corresponding author, e-mail:uday@ee.iitm.ac.in

This article has been accepted for publication in a future issue of this journal, but has not been fully edited. Content may change prior to final publication. Citation information: DOI 10.1109/TAP.2017.2715366, IEEE Transactions on Antennas and Propagation

have greatly matured in terms of their compute times [4]. We remark that the solution strategy proposed in this paper, that of using a mesh deformation technique and stochastic basis-functions/collocation-methods, can easily be incorporated into integral equation methods.

Related work: The use of a coordinate transformation technique in order to enable single-mesh Monte Carlo iterations has been recently proposed in our earlier work [5] and in [6], [7]. The probabilistic framework that we use is in light of that proposed for the solution of fluid transport in tubes with rough walls [8]. This framework utilises an analytical mapping of a deterministic differential equation defined on a random domain to a stochastic differential equation defined on a deterministic domain. Subsequently, the solution is obtained by means of a generalized Polynomial Chaos (gPC) expansion of the stochastic variables of interest and the Galerkin method (also see [9]). Similarly, in [10] the problem of wave scattering from a bounded, impenetrable object with randomly rough boundaries has been studied by suitable mapping of the Helmholtz equation to a stochastic partial differential equation. The use of a node-based FEM within the stochastic framework was originally proposed in the context of quantifying uncertainty in the mechanical responses in structures due to randomness in material properties [11]. In an electrostatics setup, a similar problem has been formulated in the case of assessing the sensitivity of electrocardiography to organ conductivity [12]. In these approaches, a stochastic character is given to a material property (corresponding to certain coefficients in the FEM equations) (also see [13] for a review). The problem that we consider is more challenging because while the material properties remain the same, the computational domain undergoes stochastic deformations. In contrast to other formulations, we use an edge-based formulation of the FEM, building on our earlier model that was recently developed for the purpose of estimating wave scattering from rough surfaces with heterogeneous soil moisture [14]. Finally, stochastic collocation methods [15], [16] have been proposed that sample intelligently from the random domain characterizing the problem, while only requiring the use of an existing deterministic solver (used in the Monte Carlo method). Depending on the dimensionality of the random domain, such methods can offer more efficient solutions than other methods, and we highlight this aspect subsequently in the text.

Outline: In Section II, we describe the mesh deformation scheme. It is readily incorporated in a Monte Carlo (MC) technique for computing ensemble averaged rough surface scattering, and we validate it against the small perturbation method. In Section III, we present the Monte Carlo-free stochastic solution to rough surface scattering; first, we review certain concepts of stochastic expansions of randomly rough surfaces, which we incorporate into the mesh deformation scheme. Next, we use the concept of gPC to construct a multivariate stochastic basis for the scattered field and perform Galerkin testing, resulting in a large system of equations. In Section IV we highlight stochastic collocation (SC) techniques; specifically, sparse grid (SG) and Stroud-3 (S3) integration rules for solving the rough surface scattering problem. Section V deals with the important issues that arise in the computation of the system of equations so obtained. Finally, in Section VI we present numerical comparisons between the Monte Carlo and stochastic approaches. After interpreting these results, we identify key implementation issues and highlight open issues.

Notation & assumptions: In this manuscript, scalars (real or complex) are denoted by lower case letters, vectors by boldface lower case letters or by symbols with an overhead arrow, and matrices by upper-case letters. In all numerical results presented, we consider transverse electric polarization, where the electric field is transverse to the computational domain.

II. Mesh deformation scheme and its validation

We propose the following smooth mesh deformation technique. Consider the schematic as shown in Fig. 1, and in particular, the shaded regions. The latter defines a 'sandwich' region which includes the interface (at $y = 0$), defined as $-h_b < y < h_t$. Next, we deform the mesh near the interface by moving all nodes within this sandwich vertically by an amount Δy in relation to the local height of the (zero mean) rough surface instance, $s(x)$, as follows:

$$\Delta y = \begin{cases} s(x)\left(\frac{h_t - y}{h_t}\right), & 0 < y < h_t \\ s(x)\left(\frac{y + h_b}{h_b}\right), & -h_b < y < 0 \end{cases} \tag{1}$$

where h_t is the maximum ordinate up to which mesh is being deformed (just below the RCS contour), and $-h_b$ is the minimum ordinate for the deformation. It is evident from Eq. (1) that mesh nodes along the smooth air-dielectric interface (i.e. $y = 0$) take the shape of the rough surface, whereas nodes outside the sandwich and on either the top or bottom-most boundary (i.e. $y = h_t, -h_b$) do not move.

We make an important remark here, that the above scheme provides a fast way of performing traditional Monte Carlo simulations of rough surface scattering, while also enabling a framework for Monte Carlo-free stochastic computations of the same problem, which we develop in Sec. III.

A. Review of the finite element method

By using first order Whitney basis functions, an edge-based formulation of the FEM equations, first order absorbing boundary conditions (along the path $A - B - F - E - A$ in Fig. (1)), and the Galerkin method [17], we arrive at a sparse, well determined system of equations in the unknown coefficients of the basis functions, $\mathbf{u}$, of the form;

$$A\mathbf{u} = \mathbf{b},\ A \in \mathbb{C}^{m\times m}, \mathbf{u}, \mathbf{b} \in \mathbb{C}^m, \text{ with,} \tag{2a}$$

$$A_{pq} = \sum_e \alpha_{e,pq}(\vec{r}_e) + \delta_{pq}\,\nu_p(\vec{r}_p), \tag{2b}$$

$$b_p = \tau_p(\vec{r}_p), \tag{2c}$$

where m is the number of edges in the domain tessellation, $\vec{r}_e$ denotes a six-tuple of the form, $(x_i, x_j, x_k, y_i, y_j, y_k)$, for the e^{th} element composed of nodes (i, j, k), $\vec{r}_p$ denotes a four-tuple of the form (x_i, x_j, y_i, y_j) for the p^{th} edge composed of nodes (i, j), $\alpha_{e,pq}$ is a function that describes the coupling between the p^{th} and q^{th} basis functions over the e^{th} element, δ_{pq} is the discrete delta function, and ν_p, τ_p are boundary integral

This article has been accepted for publication in a future issue of this journal, but has not been fully edited. Content may change prior to final publication. Citation information: DOI 10.1109/TAP.2017.2715366, IEEE Transactions on Antennas and Propagation

functions over the p^{th} edge (if it belongs to the boundary). The explicit forms of the functions α, ν, τ can be inferred by inspection of the vector FEM equation [14, Eq. 2] and the expression of the magnetic field, $\vec{H}$, in the the Whitney basis as: $\vec{H}(\vec{r}) = \sum_{i=1}^{3} u_i \vec{W}_i(\vec{r})$, where u_i is an unknown (complex) scalar to be determined, $\vec{W}_i$, is a Whitney basis function (also see Appendix A).

B. Validation with the small perturbation method

There are at least two known strategies for computing Monte Carlo averages of rough surface scattering using the FEM, and a third strategy is proposed here. In the standard approach [14], a different mesh is created for each instance of a surface realization and the above matrix equation Eq. (2) is solved each time. A more efficient technique involves using a single 'master' mesh, which is reconfigured for each instance by local modifications only in the vicinity of air-dielectric interface (see [5], or [6], [7] for related approaches).

Instead, by using the proposed mesh deformation scheme, we gain two computational advantages in comparison with the earlier schemes, in particular over [5]: (a) There is no requirement to search for the mesh nodes nearest to the interface, which leads to a significant reduction in compute time, and (b) since all nodes are nudged in a smooth fashion, no mesh element becomes skew, a phenomena which was observed to happen on rare occasion in [5].

After solving Eq. (2) for a particular instance and computing the quantities of interest, all mesh nodes are moved back to the original unperturbed positions, and the process repeated for further rough surface instances until satisfactory convergence of the Monte Carlo average is achieved.

The core FEM solver has previously been validated with analytical solutions for smooth dielectric cylinder scattering in earlier work [18]. Since the main innovation presented here pertains to the effect of rough surface scattering, we compare our results with a semi-analytical approach called the small perturbation method (SPM) which gives analytical expressions for ensemble averaged bi-static radar cross-sections [19] and is accurate for low levels of surface roughness and surface slope (a similar validation was performed in our earlier work on rough surface scattering [14]). The results of this validation are shown in Fig. (2); 100 Monte Carlo iterations took 12m45s on a 3.1GHz Intel Xeon processor consuming 400MB of RAM. There is a slight over-estimation by the SPM as compared to the FEM; this is because the standard formulation of the SPM uses plane wave excitation, whereas to prevent edge diffraction in the FEM, we use a "tapered" incident field [20].

III. Stochastic gPC approach for rough surface scattering

In this section we present a stochastic solution using gPC and Galerkin testing to the rough surface scattering problem by utilizing the mesh deformation scheme detailed earlier. We begin by reviewing some essential stochastic theory.

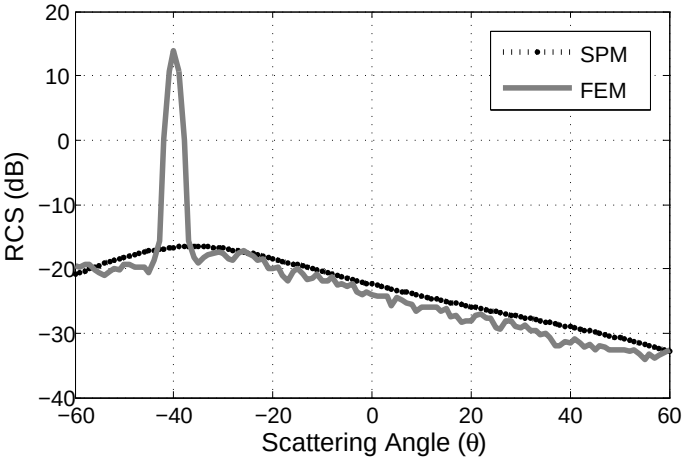

Fig. 2: Validation of rough surface scattering computed via FEM with the SPM. Note that we display first order incoherent scattering results, due to which the (coherent) peak in the specular direction is missing in comparison with the FEM. The surface length is $a = 60\lambda$, the correlation length is $l = 0.5\lambda$, and the root mean square surface roughness, h, is given by $kh = 0.1$, where $k = 2\pi/\lambda$. The substrate has a homogeneous relative permittivity: $4 - 1j$, with tapered wave incidence at 40° from the normal. The other dimensions are as per the caption of Fig. (1).

A. Review of Stochastic expansions and basis functions

Stochastic Expansion: A stochastic process, such as one describing a random interface, $\tilde{s}(x, \theta)$, can be represented by the Kosambi–Karhunen–Loève theorem (KKL) [21], [22] as an expansion in terms of the eigenfunctions $f_i(x)$ (with eigenvalue η_i) of a covariance function $C(x_1, x_2)$, and further approximated by a truncation of the expansion to d terms, as:

$$\begin{aligned} \tilde{s}(x,\theta) &= s_0(x) + \sum_{i=1}^{\infty} \sqrt{\eta_i}\, z_i(\theta)\, f_i(x) \\ &\approx s_0(x) + \sum_{i=1}^{d} \sqrt{\eta_i}\, z_i(\theta)\, f_i(x), \end{aligned} \tag{3}$$

where $s_0(x)$ is the mean height of the surface (the x-dependence can capture a tilted ground for example), $\{z_i(\theta)\}$ are zero mean, mutually uncorrelated random variables, and θ denotes random inputs in a properly defined probability space. It is known that the number of significant eigenvalues η_i in Eq. (3) decrease with an increase in the correlation length, l, and thus the truncation error decreases as the correlation length increases [23]. An exponential covariance function, $C(x_1, x_2) = \exp(|x_1 - x_2|/l)$, is chosen for two reasons; (a) many natural rough surfaces display such a covariance function [24], and (b) such a function admits to analytically expressible eigenfunctions and values [23]. The latter is only a technical convenience since eigenfunctions and values can be evaluated numerically for other covariance functions.

Stochastic basis functions: In order to find a stochastic solution to the problem of rough surface scattering, we use the concept of generalized polynomial chaos (gPC) basis

This article has been accepted for publication in a future issue of this journal, but has not been fully edited. Content may change prior to final publication. Citation information: DOI 10.1109/TAP.2017.2715366, IEEE Transactions on Antennas and Propagation

functions [25]. Univariate gPC basis functions are orthogonal polynomial functions that satisfy the following conditions;

$$\mathbb{E}[\psi_p(z_i)\psi_q(z_i)] = \int \psi_p(\theta)\psi_q(\theta)\rho(\theta)d\theta = \tilde{\psi}_p\delta_{pq}, \quad (4)$$

where $\{p,q\} \in \mathcal{N}$, $\tilde{\psi}_p$ is a normalization factor, and z_i is a random variable with finite moments and a probability distribution function (PDF), $\rho(\theta)$. Based on the above, we construct a linear space of polynomials of degree at most n, given by $\mathbb{P}_n(z_i)$, and a set of polynomials that live in this space, $\{\psi_k(z_i)\}_{k=0}^n \in \mathbb{P}_n(z_i)$, to characterize univariate gPC basis functions in z_i. Since the rough surface expansion as per Eq. (3) consists of d random variables, we employ a *multivariate* gPC expansion to derive a stochastic solution to the scattering problem. Specifically, we construct d-variate n^{th}-degree gPC functions, belonging to a space $\mathbb{P}_n^d$ of dimension $w = \binom{n+d}{n}$, which are the products of the univariate polynomials mentioned above, i.e.

$$\Psi_{\mathbf{i}}(z) = \psi_{i_1}(z_1)\dots\psi_{i_d}(z_d), \quad 0 \le |\mathbf{i}| = \sum_{j=1}^{d} i_j \le n, \quad (5)$$

where $\vec{z} = (z_1,\dots,z_d)$ is a d-dimensional random vector and $\mathbf{i} = (i_1,\dots,i_d)$ is a multi-index notation for a d-tuple. We choose Legendre polynomials as our gPC basis functions in Eq. (4) for reasons of technical convenience. With z_i being a uniform random variable in $[-1,1]$, the PDF $\rho(\theta)$ in Eq. (4) becomes constant and equal to $\frac{1}{2}$.

B. Approximations in the FEM matrix elements

To proceed towards a stochastic solution, we re-examine the matrix elements that arise for scattering from a deterministic rough surface, i.e. in Eq. (2). A particular matrix element, A_{pq}, captures the coupling between the two basis functions $\vec{W}_p$ and $\vec{W}_q$ over all the elements in common between them. This is a function of the coordinates of the three nodes of each element [17].

Next, we implement the mesh deformation on each node as per Eq. (1); since there is no $x-$shift in the nodes, the shift for each node can be expressed as $\Delta\vec{r} = (\Delta y)\hat{y}$, where $\Delta y = s(x)(1-|y|/h)$ as per Eq. (1) and $h = h_t$ (for $y > 0$) or $h = h_b$ (for $y < 0$) (with both $h_t, h_b > 0$). Accordingly, the perturbed matrix elements, $\tilde{A}_{pq}$, and $\tilde{b}_p$ can be expressed in terms of an order-expansion in $s(x)$ as follows:

$$\begin{aligned}
\tilde{A}_{pq} \approx{}& \sum_e \alpha_{e,pq}(\vec{r}_i+\Delta\vec{r}_i, \vec{r}_j+\Delta\vec{r}_j, \vec{r}_k+\Delta\vec{r}_k) \\
&+ \delta_{pq}\nu_p(\vec{r}_c+\Delta\vec{r}_c, \vec{r}_d+\Delta\vec{r}_d) \\
={}& \sum_e \{\alpha^{(0)}_{e,pq}(\vec{r}_e) + \alpha^{(1)}_{ei,pq}(\vec{r}_e)s(x_i) + \alpha^{(1)}_{ej,pq}(\vec{r}_e)s(x_j) \\
&+ \alpha^{(1)}_{ek,pq}(\vec{r}_e)s(x_k) + \alpha^{(2)}_{eij,pq}(\vec{r}_e)s(x_i)s(x_j) \\
&+ \alpha^{(2)}_{ejk,pq}(\vec{r}_e)s(x_j)s(x_k) + \alpha^{(2)}_{eki,pq}(\vec{r}_e)s(x_k)s(x_i) \\
&+ \alpha^{(2)}_{eii,pq}(\vec{r}_e)s^2(x_i) + \alpha^{(2)}_{ejj,pq}(\vec{r}_e)s^2(x_j) \\
&+ \alpha^{(2)}_{ekk,pq}(\vec{r}_e)s^2(x_k)\} \\
&+ \delta_{pq}\{\nu^{(0)}_p(\vec{r}_p) + \nu^{(1)}_{p,i}(\vec{r}_p)s(x_i) + \nu^{(1)}_{p,j}(\vec{r}_p)s(x_j)\}
\end{aligned} \quad (6a)$$

$$\tilde{b}_p = \tau^{(0)}_p(\vec{r}_p) + \tau^{(1)}_{p,i}(\vec{r}_p)s(x_i) + \tau^{(1)}_{p,j}(\vec{r}_p)s(x_j), \quad (6b)$$

where the notation is borrowed from Eq. (2), and the superscript (j) on any function denotes the order of the accompanying surface function, $s(x)$. Making the connection between the surface function and its stochastic expansion leads us to a system of equations, as demonstrated next.

C. Stochastic Galerkin method

With the spatial and stochastic basis functions fully defined, in Sec. II-A and Eq. (5), respectively, we implement an overall spatial and stochastic Galerkin procedure by expanding the unknown field, $\vec{H}(\vec{r},\vec{z})$, in composite basis functions, $\vec{\Phi}_{l,k}(\vec{r},\vec{z})$, of the form:

$$\vec{\Phi}_{l,k}(\vec{r},\vec{z}) = \vec{W}_l(\vec{r})\,\Psi_k(\vec{z}),\ 1 \le l \le m,\ 1 \le k \le w, \quad (7a)$$

$$\vec{H}(\vec{r},\vec{z}) = \sum_{l,k} \vec{\Phi}_{l,k}(\vec{r},\vec{z})\,v_{l,k} \quad (7b)$$

where the multi-index, $\mathbf{i}$, from Eq. (5) has been converted to a single index, k, and the scalars $v_{l,k}$ are the object of computation.

Further, we replace the deterministic rough surface, $s(x)$, in the matrix Eq. (6) by the stochastic counterpart, $\tilde{s}(x,\theta)$, from Eq. (3) and re-write Eq. (6) in a more convenient manner, as:

$$\tilde{A}_{pq} = \beta_{pq} + \sum_{i=1}^{d} \beta^{(i)}_{pq} z_i + \sum_{i,j=1}^{d} \beta^{(i,j)}_{pq} z_i z_j, \quad (8a)$$

$$\tilde{b}_p = \zeta_p + \sum_{i=1}^{d} \zeta^{(i)}_p z_i \quad (8b)$$

where the β_{pq}'s and η_p's, which are functions of space, can be inferred by inspection of Eqs. (6) and (8). Also note that by choosing first order Whitney basis functions, the unperturbed matrix elements β_{pq} have analytical expressions [17] and thus are very fast to compute (see Appendix A).

We now perform Galerkin testing along the same set of basis functions as Eq. (7a) (as we did in Section II), and arrive at a large, sparse, and well determined set of equations of the following form:

$$F\,\mathbf{v} = \mathbf{g},\ F \in \mathbb{C}^{mw\times mw},\ \mathbf{v},\mathbf{g} \in \mathbb{C}^{mw}, \quad (9)$$

where the vector $\mathbf{v}$, which is composed of the scalars from (7b), is solved for.

In order to visualize the matrix structure in Eq. (9), we conceptually break up F into $w \times w$ blocks. Further, we write $\mathbf{v},\mathbf{g}$ in the form: $\mathbf{v} = [\tilde{\mathbf{v}}_1,\dots,\tilde{\mathbf{v}}_w]^T$, $\mathbf{g} = [\tilde{\mathbf{g}}_1,\dots,\tilde{\mathbf{g}}_w]^T$, where $\tilde{\mathbf{v}}_k, \tilde{\mathbf{g}}_k \in \mathbb{C}^m$, and denote the corresponding $w \times w$ blocks of F as $\tilde{F}_{ab}$, where $\tilde{F}_{ab} \in \mathbb{C}^{m\times m}$. Connecting Eqs. (8) and (7a) with (9) gives:

$$\tilde{F}_{ab} = R\,E_{ab} + \sum_{i=1}^{d} R^{(i)}\,E^{(i)}_{ab} + \sum_{i,j=1}^{d} R^{(i,j)}\,E^{(i,j)}_{ab}, \quad (10a)$$

$$\tilde{\mathbf{g}}_a = \mathbf{r}\,\mathbf{e}_a + \sum_{i=1}^{d} \mathbf{r}^{(i)}\,\mathbf{e}^{(i)}_a, \quad (10b)$$

where $1 \le a,b \le w$, and :

This article has been accepted for publication in a future issue of this journal, but has not been fully edited. Content may change prior to final publication. Citation information: DOI 10.1109/TAP.2017.2715366, IEEE Transactions on Antennas and Propagation

- the E's and e's are stochastic inner products defined as: $E_{ab} = \langle \Psi_a(\vec{z}) \Psi_b(\vec{z}) \rangle$, $E_{ab}^{(i)} = \langle \Psi_a(\vec{z}) z_i \Psi_b(\vec{z}) \rangle$, $E_{ab}^{(i,j)} = \langle \Psi_a(\vec{z})\, z_i\, z_j\, \Psi_b(\vec{z}) \rangle$, $\mathbf{e}_a = \langle \Psi_a(\vec{z}) \rangle$, and $\mathbf{e}_a^{(i)} = \langle \Psi_a(\vec{z})\, z_i \rangle$. Due to the orthogonal nature of the polynomials ψ_k, many of these inner products are zero.
- the R's are matrices in $\mathbb{C}^{m \times m}$, specifically, the (p,q) elements of R, $R^{(i)}$, $R^{(i,j)}$ are β_{pq}, $\beta_{pq}^{(i)}$, $\beta_{pq}^{(i,j)}$, respectively (as per Eq. (8a)); and the $\mathbf{r}$'s are vectors in $\mathbb{C}^m$, specifically, the p-th elements of $\mathbf{r}$, $\mathbf{r}^{(i)}$ are ζ_p, $\zeta_p^{(i)}$, respectively (as per Eq. (8b)).

The evaluation of the above defined inner products is detailed in [26]. It is important to note that the R's and $\mathbf{r}$'s do not depend on the block indices $\{a,b\}$ of $\tilde{F}_{ab}$, or $\{a\}$ of $\tilde{\mathbf{g}}_a$, and hence need to be computed only once, irrespective of the degree of gPC expansion (n in Eq. (5)).

D. Computation of Radar Cross-Section

In electromagnetic scattering problems, the bi-static radar cross-section (RCS) is a primary quantity of interest. Due to the stochastic nature of the rough surface, an ensemble averaged RCS comes closer to simulating the observations of a radar than just the scattered field from a single instance of a surface, and thus the quantity of interest becomes: $\langle \sigma_{HH} \rangle = 2\pi \lim_{r \to \infty} r \langle |E^f(\vec{r}|^2 \rangle / |E^i|^2$, where $E^f(\vec{r}), E^i$ represent the $z-$component of the far-field and incident field, respectively. Note that since our problem is in two dimensions, the above definition reports a RCS-per-length quantity, also referred to as the radar echo width (REW) in the literature. By making certain assumptions (detailed in Appendix B), we express the far field as a linear combination of the field components of the edges on and neighbouring the RCS integration contour (Γ in Fig. 1):

$$E^f(\vec{r}) = \sum_{l \in \Gamma_e} \gamma_l\, u_l, \tag{11}$$

where u_l is the field component along the l^{th} edge, Γ_e is the set of all edges that belong to elements with an edge on the contour Γ, and γ_l is a geometry-dependent factor.

Having solved the large set of equations in Eq. (9), we proceed to compute the ensemble averaged RCS by taking the expectation value of the field intensity, $|E^f(\vec{r})|^2$. As discussed previously in Sec. III-C, the field associated with the l^{th} edge is replaced by the stochastic counterpart via Eq. (7b). Thus, u_l in Eq. (11) is replaced by $\sum_k \Psi_k(\vec{z}) v_{l,k}$ where $1 \leq k \leq w$.

Further, we choose to perform the deformation outlined in Sec. II such that the maximum ordinate, h_t in Eq. (1), is just short of the contour Γ (also see Fig. 1). As a result, this contour remains horizontal in all (physical or stochastic) meshes. Inspection of the explicit form of γ_l from Eq. (18) (See Appendix B) reveals that this choice of h_t greatly simplifies the algebra, as γ_l has no stochastic dependence. The stochastic far field becomes: $E^f(\vec{r}, \vec{z}) = \sum_{l \in \Gamma_e} \sum_k \gamma_l \Psi_k(\vec{z})\, v_{l,k}$, which leads to the following expression for the ensemble averaged intensity in terms of the stochastic inner products defined in Sec. III-C, Eq. (10)

$$\langle |E^f(\vec{r}, \vec{z})|^2 \rangle = \sum_{a,b \in \Gamma_e} \sum_{p,q=1}^{w} (\gamma_a^* \gamma_b)\, (v_{a,p}^* v_{b,q})\, E_{pq}. \tag{12}$$

where the stochastic inner product, E_{pq}, is as introduced in Eq. (10).

IV. Stochastic collocation approaches for rough surface scattering

Let us say that $\sigma(\vec{r}, \vec{z})$ represents the solution to the rough surface scattering problem evaluated at a spatial location $\vec{r}$ by a random rough surface characterized by a $d-$dimensional random vector, $\vec{z}$, as given by the KKL expansion in Eq. (3). The MC approach for finding the expectation value of σ is to simply average over many instances of the rough surface, i.e.

$$\langle \sigma \rangle = \sum_{i=1}^{n_{mc}} \sigma(\vec{r}, \vec{z}_i)/n_{mc}, \tag{13}$$

where n_{mc} is the number of MC iterations and $\vec{z}_i$ generates the i^{th} instance of the rough surface.

The stochastic collocation (SC) method starts by constructing a multivariate pdf of the $d-$independent random variables as $w(\vec{z}) = \prod_{j=1}^{d} w_j(z_j)$ over the tensor product domain $\mathcal{D}^d$ of the individual random variable domains, and expressing the expected value as $\langle \sigma \rangle = \int_{\mathcal{D}^d} \sigma(\vec{r}, \vec{z}) w(\vec{z}) d\vec{z}$, where $w_j(z_j)$ is the pdf of the j^{th} random variable. Next, $\sigma(\vec{x}, \vec{z})$ is expressed in terms of a basis of multivariate polynomials, $\{P^{(i)}(\vec{z})\}_{i=1}^{d}$, constructed from n_{sc} evaluations of $\sigma(\vec{r}, \vec{z})$ as: $\sigma(\vec{r}, \vec{z}) = \sum_{i=1}^{n_{sc}} \sigma(\vec{r}, \vec{z}_i) P^{(i)}(\vec{z})$, where, for instance, $P^{(i)}$ could be (but not limited to) a tensor product of univariate Lagrange interpolating polynomials. Thus, the expectation value of σ is:

$$\langle \sigma \rangle = \sum_{i=1}^{n_{sc}} \sigma(\vec{r}, \vec{z}_i) \alpha_i, \tag{14}$$

where $\alpha_i = \int_{\mathcal{D}^d} w(\vec{z}) P^{(i)}(\vec{z}) d\vec{z}$. Noting the similarity in form between Equations (13) and (14), we remark that the same deterministic solver that is used for the MC method can be used in SC approaches.

Various numerical cubature rules are used to evaluate the coefficients α_i, which depend on the form of $w(\vec{z})$ and $P^{(i)}(\vec{z})$. These range from full tensor product rules (TP) [27], to sparse grids (SG) [28], or Stroud-2/Stroud-3 (S2/S3) [29] integration rules. Each of these rules is characterized by a number n_{sc}, the set of weights α_i, and a set of specified quadrature points, $\vec{z}_i$, that can be used in Eq. (14) (see [30] for a review). In the subsequent sections, we detail the results obtained for the rough surface scattering problem when the SG or S3 integration rules are applied.

V. Computational considerations

A. On the stochastic gPC approach

The single, large, sparse matrix equation in Eq. (9) needs to be solved only once, thereby avoiding a Monte Carlo procedure. The trade off, of course, is that the resulting set of equations in Eq. (9) is larger (by a factor of w) than that encountered for a single Monte Carlo iteration as per equation Eq. (2) (of size m). Whereas a direct solution (using a LU decomposition via the open source software, MUMPS [31]) suffices for the Monte Carlo case, the same strategy fails for reasonable values of w in the case of solving the stochastic

This article has been accepted for publication in a future issue of this journal, but has not been fully edited. Content may change prior to final publication. Citation information: DOI 10.1109/TAP.2017.2715366, IEEE Transactions on Antennas and Propagation

equations (i.e. Eq. (9)) because of computational issues in storing and solving the larger system of equations.

We overcome the above computational challenge by adopting two techniques:

1) *Speed* improvement: we implement (using an open-source C++ library for linear algebra, Seldon [32]) an iterative solver based on the pre-conditioned biconjugate gradient stabilized (BiCgStab) algorithm. For the purpose of pre-conditioning — after considering the discussion on closely related problems in [33] — we implement a block-diagonal, mean-based preconditioner [34] of the form $P = \text{diag}\{R, \ldots, R\}$ where R is the matrix corresponding to a flat surface and whose elements are β_{pq} from Eq. (8a).
2) *Memory* improvement: the above solver is implemented in a "matrix free" form (using Seldon [32]), since the matrix F never needs to be stored in memory and only matrix-vector products need to be computed. Although we don't store the entire F matrix, all the R matrices ($1 + d + d^2$ in total) and $\mathbf{r}$ vectors ($1 + d$ in total) (see Eq. (10) need to be stored, which is a considerable increase in memory load as compared to the Monte Carlo case.

Parameter selection: We now discuss the physical parameters that govern m,w, and hence the computational costs incurred in solving this system of equations. Recall that m is the number of edges in the finite element tessellation of the domain and w is the size of the stochastic space.

- *Determining* m: In the horizontal direction, it is necessary for the surface to be at least several times the correlation length in order to faithfully capture the statistical properties of the surface; for exponentially correlated surfaces, this number is $a = \{12 - 25\}l$ (see Appendix C for details). With a choice of $l = \lambda$ as the correlation length, we fix the horizontal extent of our mesh to be $a = 20\lambda$. In the vertical direction, we have maintained a $1\,\lambda$ separation between the surface and the upper boundary to allow effective implementation of the radiation boundary condition [14]. The extent from the surface to the bottom boundary is determined by the depth of inhomogeneities in the domain that need to be incorporated; for the purpose of this paper, we fix this to λ. The horizontal and vertical extents having been fixed, m gets determined by well known considerations of numerical convergence of FEM equations.
- *Determining* w: The parameter w is directly determined by the choice of number of basis functions d, and their order n (both defined in Eq. (5)) with $w = \binom{n+d}{n}$. The number of basis functions, in turn, depends inversely on the correlation length of the surface (l), and directly on the length of the surface (a) [23]. In the results that we present in the following section, we fix d by allowing all eigenvalues with magnitudes greater than $\frac{1}{10}$ of the maximum eigenvalue (also see [35] and [25] for related discussions). As an illustration, some typical values based on this criteria are shown in Table I.

Thus, starting from the electrical size of the problem, and the nature of the rough surface, we arrive at the dimensionality of the overall problem in a way that can be generally applied to most electromagnetic scattering problems.

TABLE I: Number of basis functions, d, as determined by the surface length, a, and the correlation length, l. For meshes with $l = \{15, 30\}$, we have $m = \{114603, 229103\}$ respectively. All lengths are in terms of the wavelength.

$\downarrow$ l \ a$\rightarrow$	15	30
1	15	29
0.5	29	58

B. On the stochastic collocation approach

The SG integration rule needs the specification of a "level" parameter, k, [15] in order to implement Eq. (14). This parameter regulates the total degree of the multivariate polynomials, $P^{(i)}(\vec{z})$, allowed in the computation of Eq. (14). As an example, $k = 0$ corresponds to implementing a $1-$point quadrature rule in all random dimensions, and higher values of k lead to more accurate quadrature rules (Gauss-Hermite quadrature rules in this case due to the normal distribution of the random variables in the KKL expansion), but at increased computational costs. For large values of d (a case that well describes our problem), the following expression [15] gives the number of deterministic-solver evaluations required: $n_{sg} \approx 2^k \frac{d^k}{k!}$. Evidently, this number can grow very quickly with k, and soon exceed the number of evaluations required in the MC method.

The S3 integration rule is accurate if the function of interest, $\sigma(\vec{r}, \vec{z})$ in this case, can be represented by (up to) a third polynomial in $\vec{z}$. Here, the number of evaluations [29] required is given as $n_{s3} = 2d$.

Thus, the computational complexity of SC methods is established in terms of the dimensionality of the random space, d, and additionally in the case of SG, by the level parameter, k. The elegance of the SC methods is that there is no need to derive a set of coupled equations as in the case of the stochastic gPC approach, and so an existing deterministic solver can be used for solving the problem at hand.

VI. Results & Discussion

In this Section, we present numerical results and comparisons between the stochastic and Monte Carlo approaches discussed in this paper.

A. Comparing stochastic gPC and Monte Carlo methods

Numerical results: Due to the large memory requirements of the stochastic gPC method, we keep the surface length at 20λ. As per the computational considerations of eigenvalue decay mentioned in Section V, we set $d = 15$ and $n = 1$. We found that setting $n = 2$ made almost no difference to the results, but greatly increased the computational costs. In most results, the iterative (BiCGStab) solver takes between 10-28 iterations and solves the problem with a residue that is less than 10^{-10}. As for the Monte Carlo method, we find the results to have converged after 100 instances, and use this number

This article has been accepted for publication in a future issue of this journal, but has not been fully edited. Content may change prior to final publication. Citation information: DOI 10.1109/TAP.2017.2715366, IEEE Transactions on Antennas and Propagation

in our comparisons. On an Intel Xeon 3.1GHz processor, the Monte Carlo method took ≈ 950s, while the gPC method took between 1200s (10 iterations) and 2400s (28 iterations). While the memory consumption in the Monte Carlo method stayed low ($\approx 100 - 200$ MB), the stochastic method took close to 10 GB of RAM.

In Fig. (3) we show the comparison between the two methods by plotting the bi-static radar cross-section for a fixed incidence angle (40° from the normal), i.e. the behaviour of the scattered power as a function of the scattering angle. We vary the levels of surface roughness, thus covering the three regimes of interest (with $k = 2\pi/\lambda$ and h being the root mean square (rms) roughness): a good match (with $kh = 0.05$), the (approximate) point of deviation (with $kh = 0.1$), and the case when the results don't compare well (with $kh = 0.2$). We find that for $kh < 0.1$, there is a quantitative agreement between the two methods.

There are two possible causes for a lack of agreement at higher values of surface roughness.

- The first concerns the order of expansion of the perturbed matrix/vector elements (see Eq. (6)), where we adopted a second order expansion for the matrix elements, $\tilde{A}_{pq}$ and first order for the vector elements $\tilde{b}_p$ (as reflected in Eq. (8)). As the r.m.s. roughness increases, higher order terms would be required to retain accuracy of the order expansion. This of course, comes with a high computational cost; for instance, if we went upto the third order for the matrix elements, an additional d^3 (sparse) $m \times m$ matrices would need to be stored.
- The second cause is to do with the order, n, of the gPC basis functions employed being insufficient for higher values of surface roughness. Unfortunately, the relation between w, d, n is such that for a fixed value of d, going to higher values of n leads to a steep increase in w; for instance, for $d = 15, n = 1$, we have $w = 16$, whereas for $d = 15, n = 3$, we have $w = 816$ – nearly two orders of magnitude higher. In both the above possible causes, Monte Carlo based approaches would appear more favorable when faced with such high computational costs.

Finally, we would like to emphasize that one of the primary objectives of this paper is a proof of concept of the Monte Carlo and stochastic–solution approaches, and our implementation of the gPC is far from being optimal. The memory requirements can be greatly reduced by implementing the stochastic solver with support for sparse vectors. Further, since both the approaches fall under the category of "embarrassingly parallel" algorithms, the processor time can similarly be reduced by parallelizing the code. For instance, in Eqn. (10), the component matrices that make up F_{ab}, i.e. $E_{ab}, E_{ab}^{(i)}, E_{ab}^{(i,j)}, R^{(i)}, R^{(i,j)}$ can all be evaluated independently on separate processors due to their independence. Further, in implementing the solution to the system of equations in Eqn. (9), the matrix-vector product that requires computation is composed of the multiplication of a $w \times w$ block matrix by a $w \times 1$ block vector. Each of these blocks can be computed on a separate processor in order to speed up the overall computation. These, and other computational optimizations are part of ongoing work.

The curse of dimensionality: The above discussion naturally leads to a more general discussion of the applicability of the stochastic gPC method. In the endeavor to cast a deterministic set of scattering equations into a stochastic form, the key step was the KKL expansion of the surface as an eigen expansion. We plot the eigenvalues in Fig. (4) for a series of surfaces with different correlation lengths. This figure uncovers an important limitation of the stochastic method; since the eigenvalues decay gradually for smaller correlation lengths, we would require higher and higher number of eigen functions in the KKL expansion to represent the surface accurately (i.e. d), thus increasing the computational load to a point where MC methods win over (also see Table I). On the other hand, the stochastic method wins over for surfaces with long correlation lengths since the convergence of MC methods typically goes as $O(\frac{1}{\sqrt{N}})$ (N is the number of iterations. While the computational cost of stochastic gPC methods becomes prohibitive as d increases, stochastic collocation techniques offer an interesting alternative to MC methods depending on the problem parameters and we discuss these next.

B. Comparing stochastic collocation and Monte Carlo methods

It is found by taking several examples that the range for d in order to accurately represent rough surfaces is $15 - 100$, for the range of surface correlation lengths considered in this text. In the SG method, for $k = 1, 2$ we get $n_{sg} \approx 2d, 2d^2$, respectively, while we have $n_{s3} = 2d$ for the S3 method. On the other hand, the number of evaluations required in the MC method is independent of d, and we find that $n_{mc} \approx 100$ evaluations are sufficient for convergence. Thus, for all practical cases, $k = 1$ is the only SG level that can be competitive to the MC method.

We compared the results of SG and S3 with those obtained by the MC method for an extensive range of parameters of surface rms roughness and correlation length, and show a subset of the results in Fig. (5) We find that;

- At low levels of surface roughness, all four methods (gPC,SG,S3,MC) agree. Within these surfaces, for those with a higher correlation length, (SG/S3) require lesser number of iterations as compared to MC and therefore are optimal, because a lower d is sufficient to characterize the surface.
- As the mean roughness of the surfaces increases, the agreement of SG/S3 with MC only remains for those with a higher correlation length. To make the agreement better, the dimensionality of the random space (d) must be increased, and this is seen in Fig. (5), where going from $d = 20$ to $d = 50$ results in an excellent match between SC and MC results. However, beyond a point, this quickly leads to a higher number of iterations for SC as compared to MC, thus negating the advantage gained.
- Rough surface scattering is often a problem characterized by a large number of random variables (typically $d > 50$), and for such cases MC is the preferred approach. For

This article has been accepted for publication in a future issue of this journal, but has not been fully edited. Content may change prior to final publication. Citation information: DOI 10.1109/TAP.2017.2715366, IEEE Transactions on Antennas and Propagation

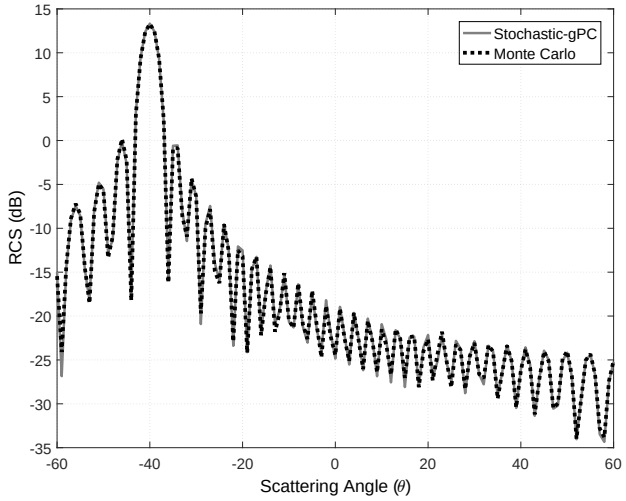

(a) $kh = 0.05$

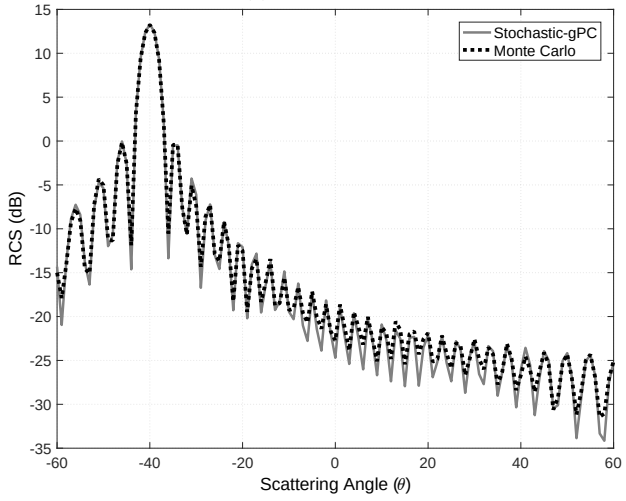

(b) $kh = 0.1$

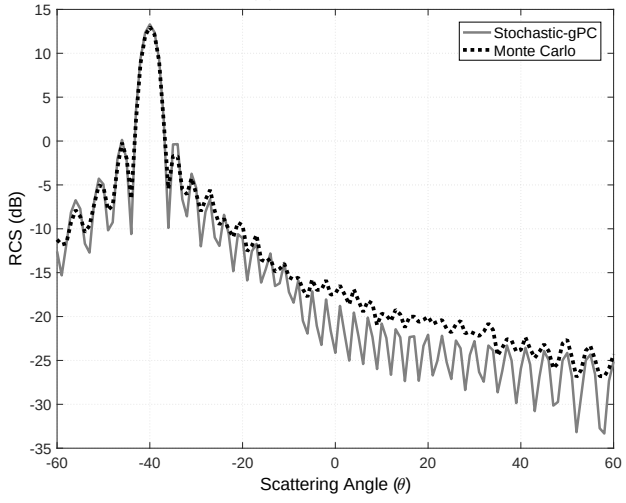

(c) $kh = 0.2$

Fig. 3: Comparison between stochastic gPC and Monte Carlo results for various values of rms surface roughness, h. For all figures, the surface length is 20λ, while the correlation length is λ. The substrate has a homogeneous relative permittivity: $4 - 1j$, with wave incidence at 40° from the normal.

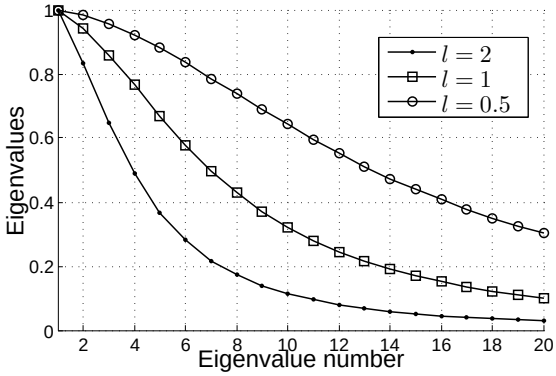

Fig. 4: Decay of (normalized) eigenvalues from the KKL expansion as a function of correlation length, l, for a surface length, $a = 20$. All lengths normalized to wavelength.

those cases where a lower number of random variables are accurate in characterizing the problem (typically $d < 20$ found for highly correlated surfaces), stochastic methods will win over the Monte Carlo method.

In summary, we can say that in any scattering problem, a careful study of the correlation length and r.m.s. roughness of the stochastic process is key to choosing the right solution approach. The earlier discussion on the 'curse of dimensionality' with regards to the stochastic gPC method is well appreciated in the literature [33]. The idea that the actual quantity of interest (the RCS in our case) can be quantified by a lower dimensional basis even though it is embedded inside a much higher dimensional space has spawned recent work relating to 'dimensionality reduction' [36]–[38]. In the case of stochastic collocation methods, the use of adaptive sparse grids [39], [40] is being seen as a way of out-performing Monte Carlo methods. These and other methods are an active area of research.

Role of incident field: Since the scattering object is a half-space and therefore unbounded, care needs to be taken in the choice of the incident field. Choosing a plane wave has a characteristic feature of producing a sinc-like diffraction pattern due to uniform illumination of a finite surface. A common alternative is to use a "tapered" wave with a gaussian amplitude profile [20], which is an approximate solution to Maxwell's equations. Although detailed studies on the determination of the optimal width of this taper have been done [41], including such an incident field is beyond the scope of the present paper. This is because computational load increases due to the need for a longer surface (i.e. m increases), since it is necessary to include several correlation lengths within the beam width for numerical convergence of the results. Note that this is not an issue in the case of Monte Carlo simulations [14], where the memory requirements are on the order of a single (sparse) $m \times m$ matrix, whereas in the stochastic case it is on the order of $1 + d + d^2$ (sparse) $m \times m$ matrices.

Postscript: We acknowledge a technical problem in comparing the results obtained by the two different approaches outlined in the paper in Sections II and III, respectively. In the stochastic gPC approach of Section III, we find that since the underlying probability distribution function is not Gaussian

This article has been accepted for publication in a future issue of this journal, but has not been fully edited. Content may change prior to final publication. Citation information: DOI 10.1109/TAP.2017.2715366, IEEE Transactions on Antennas and Propagation

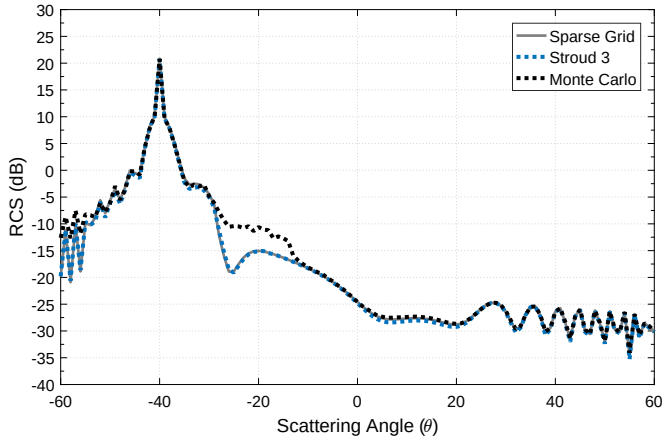

(a) $d = 20$

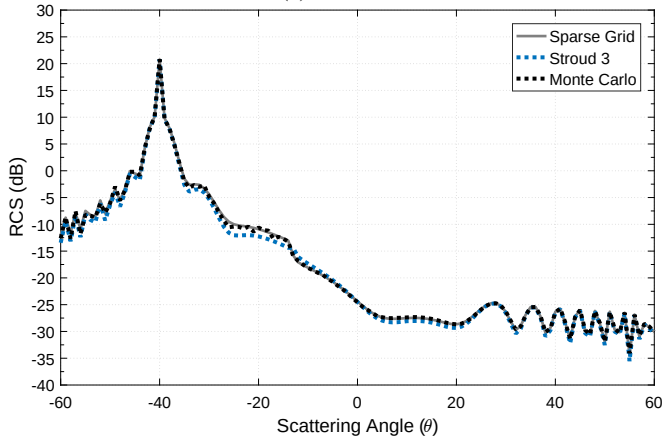

(b) $d = 50$

Fig. 5: Comparison between stochastic collocation and Monte Carlo results for two values of random dimensionality, d. For all figures, the surface length is 60λ, rms surface roughness, $kh = 0.2$ while the correlation length is 5λ. The substrate has a homogeneous relative permittivity: $4 - 1j$, with plane wave incidence at 40° from the normal.

in the case of Lengendre polynomials, the prescription from Eq. (4) leads to uncorrelation of the random variables, but this does not imply independence. A Monte-Carlo based solution to the rough surface scattering problem would entail implementing Eq. (3) to generate an instance of a rough surface. Now, pseudo-random number generators produce (nearly) independent random variables. However, as discussed, the choice of Legendre polynomials in a stochastic gPC approach to the same problem now leads to random variables $\{z_i\}$ that are not independent. Thus, a comparison between the results of these two approaches is not expected to exactly coincide. This issue has been identified in the literature [25], [42], [43], and continues to be an area of active research. Ascertaining the exact contribution due to this effect alone is difficult, since other factors such as those identified above (order of stochastic expansion, r.m.s. roughness, etc.) simultaneously contribute to the overall solution. At least from the study of scattering by low roughness surfaces (e.g. Fig. (3a)), where the solution matches the Monte Carlo results exactly, this effect does not seem to have any appreciable impact. Further, we note that this issue does not affect the stochastic collocation methods since no expansion in the basis of orthogonal polynomials w.r.t. some pdf is involved.

ACKNOWLEDGEMENTS

UKK gratefully acknowledges discussions with Oscar P Bruno (Caltech) on the mesh deformation scheme, and with Thomas Cwik (Jet Propulsion Laboratory) on the stochastic galerkin method. UKK acknowledges support by the INSPIRE Faculty Award (IFA-13 ENG-60) from the Department of Science and Technology, Government of India. The authors also acknowledge helpful comments from the reviewers which went a long way in improving the quality of the manuscript.

APPENDIX A
FINITE ELEMENT MATRIX COEFFICIENTS

The unperturbed matrix and vector coefficients, $\beta_{pq}(x_i, x_j, x_k, y_i, y_j, y_k) \equiv \beta_{pq}$ and ζ_p, respectively, are defined as [17]:

$$\beta_{pq} = \sum_{e}^{(i,j,k)} \frac{l_p l_q}{\Delta}\Big(\frac{1}{\epsilon_r} + \frac{k_0^2\mu_r}{24}(x_i^2 - x_j^2 + x_k^2 - 3x_i x_k + x_i x_j + x_j x_k + y_i^2 - y_j^2 + y_k^2 - 3y_i y_k + y_i y_j + y_j y_k)\Big) - \delta_{pq} l_p$$

$$\beta_{pp} = \sum_{e}^{(i,j,k)} \frac{l_p^2}{\Delta}\Big(\frac{1}{\epsilon_r} - \frac{k_0^2\mu_r}{24}(x_i^2 + x_j^2 + 3x_k^2 - 3x_i x_k + x_i x_j - 3x_j x_k + y_i^2 + y_j^2 + 3y_k^2 - 3y_i y_k + y_i y_j - 3y_j y_k)\Big) - jk_0 l_p$$

$$\zeta_p = \left[jk_0 E_{iz} + \frac{1}{\sqrt{\epsilon_r\mu_r}}\Big(n_x\frac{\partial E_{iz}}{\partial x} + n_y\frac{\partial E_{iz}}{\partial y}\Big)\right]\frac{l_p}{Z_0}$$

where $\Delta = \frac{1}{2}(y_i(x_k - x_j) + y_j(x_i - x_k) + y_k(x_j - x_i))$, and edge p (length l_p) is composed of nodes $\{i, j\}$ (i.e. edge i per our convention), edge q (length l_q) of nodes $\{j, k\}$ (i.e. edge j), $\hat{n} = (n_x, n_y, 0)$ is the outward normal to outer-most contour above the ground, and E_{iz} is the magnitude of the $z-$polarized incident electric field.

In β_{pq}, for a perturbation in the y's as $y_i \to y_i + \delta_i$ with $\delta_i = s(x_i)(1 - |y_i|/h)$, and $s(x_i) = \sum_{a=1}^{d}\sqrt{\eta_a} f_a(x_i) z_a$, we get the following multi-variable Taylor expansion (upto order two for β_{pq} and order one for ζ_p):

$$\beta_{pq}(y + \delta) \approx \beta_{pq} + \sum_{i,j,k}\delta_i\frac{\partial\beta_{pq}}{\partial y_i} + \sum_{\{i,j\}}\frac{\delta_i\delta_j}{2}\frac{\partial^2\beta_{pq}}{\partial y_i\partial y_j}$$

$$\zeta_p(y + \delta) \approx \zeta_p + \sum_{i,j}\delta_i\frac{\partial\zeta_p}{\partial y_i}$$

For Eq. (8a), i.e. $\tilde{A}_{pq} = \beta_{pq} + \sum_{a=1}^{d}\beta_{pq}^{(a)} z_a + \sum_{a,b=1}^{d}\beta_{pq}^{(a,b)} z_a z_b$, and for Eq. (8b), i.e. $\tilde{\zeta_p} = \zeta_p + \sum_{a=1}^{d}\zeta_p^{(a)} z_a$, we can simply the expressions as:

This article has been accepted for publication in a future issue of this journal, but has not been fully edited. Content may change prior to final publication. Citation information: DOI 10.1109/TAP.2017.2715366, IEEE Transactions on Antennas and Propagation

$$\beta_{pq}^{(a)} = \sum_e \sum_{i,j,k} \left(1 - \frac{|y_i|}{h}\right) \sqrt{\eta_a} f_a(x_i) \frac{\partial \beta_{pq}}{\partial y_i}$$

$$\beta_{pq}^{(a,b)} = \sum_e \sum_{\{i,j\}} \frac{1}{2}(1 - \frac{|y_i|}{h})(1 - \frac{|y_j|}{h}) \sqrt{\eta_a \eta_b} f_a(x_i) f_b(x_j) \frac{\partial^2 \beta_{pq}}{\partial y_i \partial y_j}$$

$$\zeta_p^{(a)} = \sum_{i,j} \left(1 - \frac{|y_i|}{h}\right) \sqrt{\eta_a} f_a(x_i) \frac{\partial \zeta_p}{\partial y_i}$$

We choose to implement these partial derivatives numerically using a central difference scheme, though they can be evaluated analytically in certain cases.

Appendix B
Radar Cross-Section computation details

By making a piece-wise constant approximation for the integral that arises in Huygen's principle for computation of the scattered far field [44], and using the first order Whitney basis functions for the magnetic field [17], we get the following expression (for H-pol);

$$E^f(\vec{r}) = \sqrt{\frac{k_0}{8\pi r}} \exp[j(\frac{\pi}{4} - k_0 r)] \sum_{l \in \Gamma} [\sin(\phi_l - \theta_s) E_{zl} - Z_0 \mu_r H_{tl}] \exp[j k_0 r' \cos(\psi_l - \theta_s)] l_l \quad (16)$$

where θ_s, ϕ_l are geometry dependent factors as denoted in Fig. 6, and H_{tl}, E_{zl} represent the tangential (in a counter clockwise sense) and z-component of the magnetic and electric field along the l^{th} edge, respectively. The latter can be written as an average over the elements (denoted by superscript e below) on either side of Γ as

$$E_{zl} = \frac{jZ_0}{2k_0} \sum_{e=1}^{2} \frac{1}{\Delta_e \epsilon_r^e} \sum_{l=1}^{3} l_l^e u_l^e. \quad (17)$$

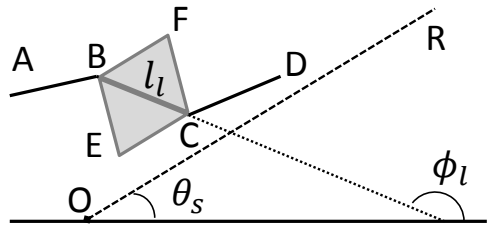

Fig. 6: Schematic for RCS computation. Part of the surface is denoted by the line segments $ABCD$ (corresponding to Γ). The finite elements accompanying the edge BC are shown in shaded-gray; the addition of the other edges of these elements, such as BF, FC, CE, BE to the set Γ constitutes the set Γ_e. The radar receiver is in the far-field at the point R with polar angle θ_s, while the edge BC with length l_l has a polar angle ϕ_l.

Note that the above expression immediately links the l^{th} edge on Γ to four other edges that are not on Γ, thus motivating the set of edges denoted as Γ_e, which includes such edges in addition to those on Γ. The above can be substituted into (16) to obtain $E^f(\vec{r}) = \sum \gamma_l u_l$ for $l \in \Gamma_e$, i.e. Eq. (11), and $\gamma_l = \gamma_l' \sqrt{k_0/(8\pi r)} \exp[j(\frac{\pi}{4} - k_0 r)]$, where γ_l' is given by

$$\gamma_l' = \begin{cases} \left[\frac{jZ_0 l_l}{4k_0} \sin(\phi_l - \theta_s)(\sum_{e=1}^{2} \frac{2}{\Delta_e \epsilon_r^e}) - Z_0 \mu_r\right] \times & \text{if } l \in \Gamma \\ \quad l_l \exp[j k_0 r' \cos(\psi_l - \theta_s)], & \\ \left[\frac{jZ_0 l_l}{2k_0 \Delta} \sin(\phi_k - \theta_s) \left(\frac{1}{\epsilon_r^e}\right)\right] \times & \text{if } l \in \Gamma_e, \notin \Gamma \\ \quad l_k \exp[j k_0 r' \cos(\psi_k - \theta_s)], & \end{cases} \quad (18)$$

where k in the second case (when $l \in \Gamma_e, \notin \Gamma$) refers to that edge of the common element e, which is on Γ.

Appendix C
Required surface length for a correlated rough surface

Consider a surface with a correlation function of the type $C(\tau) = \sigma^2 \exp(-|\tau/l|^n)$, where l is the correlation length and $n = 1, 2$ correspond to exponential and gaussian correlation functions, respectively. In order to generate an instance of a rough surface (see [20] for a scheme), we first compute the Fourier transform of this auto correlation function, $W(k)$. We limit $C(\tau)$ by some parameter $\tau = \tau_{\max}$ so that the Nyquist sampling theorem can be used to evaluate $W(k)$ with a sampling rate $1/\Delta k \geq 2\tau_{\max}$. Now, we choose $\tau_{\max}$ such that $C(\tau_{\max})/C(\tau) = 1/\gamma \ll 1$. Together with $\Delta k = 2\pi/a$, where a is the surface length, we get (after some algebra): $l/a = (4\pi/n) \ln \gamma$. Thus, for exponentially correlated surfaces a choice for γ such as $e < \gamma < e^2$ gives a suitable range for l as $4\pi < l/a < 8\pi$.

References

[1] D. Entekhabi, E. G. Njoku, P. E. O'Neill, K. H. Kellogg, W. T. Crow, W. N. Edelstein, J. K. Entin, S. D. Goodman, T. J. Jackson, J. Johnson *et al.*, "The soil moisture active passive (smap) mission," *Proceedings of the IEEE*, vol. 98, no. 5, pp. 704–716, 2010.

[2] K. F. Warnick and W. C. Chew, "Numerical simulation methods for rough surface scattering," *Waves in Random Media*, vol. 11, no. 1, pp. R1–R30, 2001.

[3] P. S. Narvekar, D. Entekhabi, S.-B. Kim, and E. G. Njoku, "Soil moisture retrieval using l-band radar observations," *IEEE Transactions on Geoscience and Remote Sensing*, vol. 53, no. 6, pp. 3492–3506, 2015.

[4] W. C. Chew, M. S. Tong, and B. Hu, "Integral equation methods for electromagnetic and elastic waves," *Synthesis Lectures on Computational Electromagnetics*, vol. 3, no. 1, pp. 1–241, 2008.

[5] U. K. Khankhoje and T. A. Cwik, "A mesh reconfiguration scheme for speeding up monte carlo simulations of electromagnetic scattering by random rough surfaces," *Computer Physics Communications*, vol. 185, no. 2, pp. 445–447, 2014.

[6] O. Ozgun and M. Kuzuoglu, "A transformation media based approach for efficient monte carlo analysis of scattering from rough surfaces with objects," *IEEE Transactions on Antennas and Propagation*, vol. 61, no. 3, pp. 1352–1362, 2013.

[7] M. Kuzuoglu and O. Ozgun, "Combining perturbation theory and transformation electromagnetics for finite element solution of helmholtz-type scattering problems," *Journal of Computational Physics*, vol. 274, pp. 883–897, 2014.

[8] D. M. Tartakovsky and D. Xiu, "Stochastic analysis of transport in tubes with rough walls," *Journal of Computational Physics*, vol. 217, no. 1, pp. 248–259, 2006.

[9] D. Xiu and D. M. Tartakovsky, "Numerical methods for differential equations in random domains," *SIAM Journal on Scientific Computing*, vol. 28, no. 3, pp. 1167–1185, 2006.

[10] D. Xiu, J. Shen *et al.*, "An efficient spectral method for acoustic scattering from rough surfaces," *Commun. Comput. Phys*, vol. 1, pp. 54–72, 2007.

This article has been accepted for publication in a future issue of this journal, but has not been fully edited. Content may change prior to final publication. Citation information: DOI 10.1109/TAP.2017.2715366, IEEE Transactions on Antennas and Propagation

[11] P. D. Spanos and R. Ghanem, "Stochastic finite element expansion for random media," *Journal of engineering mechanics*, vol. 115, no. 5, pp. 1035–1053, 1989.

[12] S. E. Geneser, R. M. Kirby, and R. S. MacLeod, "Application of stochastic finite element methods to study the sensitivity of ecg forward modeling to organ conductivity," *IEEE Transactions on Biomedical Engineering*, vol. 55, no. 1, pp. 31–40, 2008.

[13] G. Stefanou, "The stochastic finite element method: past, present and future," *Computer Methods in Applied Mechanics and Engineering*, vol. 198, no. 9, pp. 1031–1051, 2009.

[14] U. K. Khankhoje, J. J. van Zyl, and T. A. Cwik, "Computation of radar scattering from heterogeneous rough soil using the finite-element method," *Geoscience and Remote Sensing, IEEE Transactions on*, vol. 51, no. 6, pp. 3461 – 3469, June 2013.

[15] D. Xiu and J. S. Hesthaven, "High-order collocation methods for differential equations with random inputs," *SIAM Journal on Scientific Computing*, vol. 27, no. 3, pp. 1118–1139, 2005.

[16] I. Babuška, F. Nobile, and R. Tempone, "A stochastic collocation method for elliptic partial differential equations with random input data," *SIAM Journal on Numerical Analysis*, vol. 45, no. 3, pp. 1005–1034, 2007.

[17] J.-M. Jin, *The finite element method in electromagnetics*. John Wiley & Sons, 2014.

[18] P. Shah, U. K. Khankhoje, and M. Moghaddam, "Inverse scattering using a joint l1-l2 norm-based regularization," *IEEE Transactions on Antennas and Propagation*, vol. 64, no. 4, pp. 1373–1384, April 2016.

[19] S. O. Rice, "Reflection of electromagnetic waves from slightly rough surfaces," *Communications on pure and applied mathematics*, vol. 4, no. 2-3, pp. 351–378, 1951.

[20] E. I. Thorsos, "The validity of the kirchhoff approximation for rough surface scattering using a gaussian roughness spectrum," *Acoustical Society of America Journal*, vol. 83, pp. 78–92, Jan. 1988.

[21] D. Kosambi, "Statistics in function space," *J. Indian Math. Soc*, vol. 7, no. 1, pp. 76–88, 1943.

[22] M. Loève, "Probability theory. 1977," 1977.

[23] H. L. Van Trees, *Detection, estimation, and modulation theory, Part 1*. John Wiley & Sons, 1968.

[24] J. Shi, J. Wang, A. Y. Hsu, P. E. O'Neill, and E. T. Engman, "Estimation of bare surface soil moisture and surface roughness parameter using l-band sar image data," *IEEE Transactions on Geoscience and Remote Sensing*, vol. 35, no. 5, pp. 1254–1266, 1997.

[25] D. Xu, "Numerical methods for stochastic computations," 2010.

[26] H. Hakula and M. Leinonen, "On efficient construction of stochastic moment matrices," *arXiv preprint arXiv:1502.07562*, 2015.

[27] P. J. Davis and P. Rabinowitz, *Numerical integration*. Blaisdell publishing company London, 1967.

[28] S. A. Smolyak, "Quadrature and interpolation formulas for tensor products of certain classes of functions," in *Dokl. Akad. Nauk SSSR*, vol. 4, no. 240-243, 1963, p. 123.

[29] A. H. Stroud, *Approximate calculation of multiple integrals*. Prentice-Hall, 1971.

[30] A. C. Yucel, "Uncertainty quantification for electromagnetic analysis via efficient collocation methods," Ph.D. dissertation, The University of Michigan, 2013.

[31] P. R. Amestoy, I. S. Duff, J.-Y. L'Excellent, and J. Koster, "A fully asynchronous multifrontal solver using distributed dynamic scheduling," *SIAM Journal on Matrix Analysis and Applications*, vol. 23, no. 1, pp. 15–41, 2001.

[32] "Seldon c++ library for linear algebra," http://seldon.sourceforge.net/, accessed: 2016-06-30.

[33] R. Tipireddy, *Algorithms for stochastic Galerkin projections: Solvers, basis adaptation and multiscale modeling and reduction*. University of Southern California, 2013.

[34] C. E. Powell and H. C. Elman, "Block-diagonal preconditioning for spectral stochastic finite-element systems," *IMA Journal of Numerical Analysis*, vol. 29, no. 2, pp. 350–375, 2009.

[35] H. Li and D. Zhang, "Probabilistic collocation method for flow in porous media: Comparisons with other stochastic methods," *Water Resources Research*, vol. 43, no. 9, 2007.

[36] A. Doostan and H. Owhadi, "A non-adapted sparse approximation of pdes with stochastic inputs," *Journal of Computational Physics*, vol. 230, no. 8, pp. 3015–3034, 2011.

[37] C. Schwab and C. J. Gittelson, "Sparse tensor discretizations of high-dimensional parametric and stochastic pdes," *Acta Numerica*, vol. 20, pp. 291–467, 2011.

[38] R. Tipireddy and R. Ghanem, "Basis adaptation in homogeneous chaos spaces," *Journal of Computational Physics*, vol. 259, pp. 304–317, 2014.

[39] F. Nobile, R. Tempone, and C. G. Webster, "An anisotropic sparse grid stochastic collocation method for partial differential equations with random input data," *SIAM Journal on Numerical Analysis*, vol. 46, no. 5, pp. 2411–2442, 2008.

[40] X. Ma and N. Zabaras, "An adaptive hierarchical sparse grid collocation algorithm for the solution of stochastic differential equations," *Journal of Computational Physics*, vol. 228, no. 8, pp. 3084–3113, 2009.

[41] H. Ye and Y.-Q. Jin, "Parameterization of the tapered incident wave for numerical simulation of electromagnetic scattering from rough surface," *IEEE transactions on antennas and propagation*, vol. 53, no. 3, pp. 1234–1237, 2005.

[42] K. Phoon, S. Huang, and S. Quek, "Simulation of second-order processes using karhunen–loeve expansion," *Computers & structures*, vol. 80, no. 12, pp. 1049–1060, 2002.

[43] S. Sakamoto and R. Ghanem, "Polynomial chaos decomposition for the simulation of non-gaussian nonstationary stochastic processes," *Journal of engineering mechanics*, vol. 128, no. 2, pp. 190–201, 2002.

[44] A. F. Peterson, S. L. Ray, R. Mittra, I. of Electrical, and E. Engineers, *Computational methods for electromagnetics*. IEEE press New York, 1998, vol. 2.

Uday K Khankhoje (M'14-SM'16) is an Assistant Professor of Electrical Engineering at the Indian Institute of Technology Madras, India. He received a B.Tech. degree from the Indian Institute of Technology Bombay, India, in 2005, an M.S. and Ph.D. degrees from the California Institute of Technology, Pasadena, USA, in 2010, all in Electrical Engineering. He was a Caltech Postdoctoral Scholar at the Jet Propulsion Laboratory (NASA/Caltech) from 2011-2012, a Postdoctoral Research Associate in the Department of Electrical Engineering at the University of Southern California, Los Angeles, USA, from 2012-2013, and an Assistant Professor of Electrical Engineering at the Indian Institute of Technology Delhi, India from 2013-16. His research interests lie in the area of computational electromagnetics and its applications to remote sensing and inverse imaging.

Shreyas Padhy is a Senior Undergraduate student in the Department of Physics at the Indian Institute of Technology Delhi, New Delhi, India. His research interests lie in the areas of medical image computing and inverse problems.